Polymer 49 (2008) 4462–4468

Contents lists available at ScienceDirect

Polymer

journal homepage: www.elsevier.com/locate/polymer

Strain inhomogeneity effect on yielding of polymer nanocomposites

G. Spathis, E. Kontou*

School of Applied Mathematical and Physical Sciences, Section of Mechanics, National Technical University of Athens, 5 Heroes of Polytechnion, GR-15773 Athens, Greece

ARTICLE INFO

Article history:
Received 4 July 2008
Received in revised form 23 July 2008
Accepted 24 July 2008
Available online 30 July 2008

Keywords:
Free volume distribution
Yielding
Glassy state

ABSTRACT

In this work, yielding and post yielding effects are analyzed using the idea of the inhomogeneous distribution of strain in polymers under deformation. This idea is directly connected with the free volume concept, as created in the polymeric bulk during the frozen in process, and or the density fluctuations combined with other type defects. A simple strain density distribution function is assumed, following experimental results available from techniques such as positron annihilation lifetime spectroscopy (PALS). Hereafter, a functional form of the rate of plastic deformation is extracted, which will be combined with a given kinematic formulation. The proposed analysis is tested with experimental data of polystyrene (PS) and PS/SiO_2 nanocomposites. The incorporation of nanosized fillers into the polymeric bulk, strongly affects the free volume distribution and/or the distribution of defects related with density fluctuations. This fact is reflected in the model parameter values, and their variation in respect to the different material types. With the proposed analysis, it has been proved that all features of yield process, including strain softening and strain hardening effect are easily described.

1. Introduction

Glassy polymers, when subjected to a sufficiently high stress field, undergo permanent deformation. This plastic deformation or yielding is manifested by a stress peak, which is followed by a stress softening, and hereafter strain hardening. Yielding is affected by the imposed strain rate, temperature and pressure conditions as well as thermal prehistory. For that reason yielding of glassy polymers has been the subject of a lot of works, which are based both on continuum mechanics in large deformations and on micromechanics modeling [1–7]. The yield behaviour of representative glassy polymers, such as polystyrene, polymethylmethacrylate and polycarbonate has been extensively examined [6–8]. Two main categories of theories, based either on viscous flow or plastic deformation in metals are usually applied for the description of polymer's yielding. The earliest models proposed that yield occurs by liquid-like flow when adiabatic heating raises the local temperature to T_g, or when tensile strain increases the free volume sufficiently [9]. Considering that the glassy state is a supercooled liquid, the deformation process can be treated as a molecular process that mainly occurs above T_g. Such a large-scale diffusion motion is generally inconsistent with intrinsic strain softening and subsequent strain localization. However, under the combined influence of stress and thermal energy the plastic strain rate is determined by the Eyring concept [10]. A lot of treatments for yielding in glassy polymers have been applied in this concept. Referring to models that employ molecular scale deformation of polymer chains to account for yield, attention must be paid to Argon's theory, that deals explicitly with intermolecular resistance to shear yielding [3].

This analysis couples bond rotation (kink pair formation) to intermolecular energy calculated with continuum elasticity theory, and has the macroscopic yield stress related directly with temperature and strain rate. The Argon results closely resemble the Eyring [10] model, which considers plastic transformation as a thermal activated process, but its special formulation leads to temperature and rate dependencies that are virtually indistinguishable from Eyring approach. The important conclusion that resistance to plastic deformation at the yield point is intermolecular in origin does not account, however, in an obvious way for strain softening. To overcome this, BPA model [5] was introduced, where Argon's concept of athermal strength has been varied by an empirical equation as plastic deformation proceeds. Later, Hasan and Boyce [7], trying to capture all plasticity features of amorphous polymers including temperature treatments, developed a constitutive model, by considering a distribution in the activation energy barrier to deformation in a thermally activated model of yielding process. In their treatment, a plausible assumption of "pseudo-Gaussian" distribution of activated energy barriers is made, which is based on a similar distribution of the amount and size of free volume holes inside the substance of amorphous polymers. Yield and free volume concept are historically associated inspite of the fact that the latter has been doubted many times [9]. Positron annihilation lifetime spectroscopy (PALS) [8]

* Corresponding author. Tel.: +30 210772129; fax: +30 2107721302.
E-mail address: ekontou@central.ntua.gr (E. Kontou).

0032-3861/$ – see front matter © 2008 Elsevier Ltd. All rights reserved.
doi:10.1016/j.polymer.2008.07.039

was been used to probe free volume in liquid and glassy polymers. This method provides unique information about the properties of subnanometer size local free volume (holes) appearing due to the structural disorder in amorphous polymers [11]. Through this technique, the mean value and the size distribution of these holes can be estimated. These values, when combined with pressure–volume–temperature experiments, can lead to the calculation of the number of holes and their entire volume fraction [12–15].

In the present work, the concept of free volume and or density/defect's fluctuations will be the basic idea for a constitutive description of yielding in glassy polymers. It will be shown that not only the amount of free volume but also the way it is distributed within the bulk material plays a decisive role during yielding of glassy state. The distributed nature of free volume (defects) will be related with the strain distribution and finally with the rate of plastic deformation. Based on this idea, which as abovementioned, was initially applied by Hasan and Boyce [7], we introduce a density distribution function for the imposed strain on the representative volume of deformed material. In this way the strain inhomogeneity, that is established during plastic deformation, will be taken into account and as it will be shown the subsequent strain softening effect can also be described. This can be achieved in the frame of a proper kinematic formulation. For this reason, we will avoid the common kinematic plastic formulation of multiple decomposition of deformational tensor, which does not take into account the advantage of strain inhomogeneity across the representative volume element. Instead of this, the kinematic formulation introduced by Rubin [16,17] will be applied. This theory, initially proposed for crystalline materials, has been successfully applied to describe the yield response of amorphous glassy polymers [18,19]. Our analysis has been confirmed with the experimental results of pure polystyrene (PS) and a series of PS/SiO_2 nanocomposites. The incorporation of nanofillers into the bulk matrix creates a different free volume (or defects) distribution; so the materials studied, are of similar structure, however, a different degree of homogeneity is expected. Tensile and compressive results of pure PS and PS/SiO_2 at three different weight fractions were performed at temperature of 85 °C, where the viscoplastic response of the materials is manifested. The simulated results appear to have a very good agreement with the experimental data, while the same set of parameters has been used for both types of experiments.

2. Free volume distribution

Several experimental methods indicate that the amorphous glassy state is not homogeneous at the microscopic level. Small-angle X-ray scattering technique proved to be a convenient way of determining density fluctuation of amorphous polymers in liquid and glassy state, and its utility in the study of glassy polymer was first demonstrated by Wendorff et al. [20]. Curro and Roe [21], on the other hand, utilized the technique of X-ray scattering to correlate the change of the specific volume with that in the density fluctuation, for three widely used polymers (PS, PMMA, PC). Following their experimental data Curro and Roe [22] derived an equation which relates explicitly the density fluctuation of glassy state with the free volume fraction (or hole volume) in amorphous polymers. Considering the value of 0.025 for the free volume fraction (valid for a wide variety of polymers through the WLF equation [23]), they estimate the cavity size in glassy polymers ($\approx$0.5 nm in diameter), which is in agreement with data on the positron annihilation lifetime spectroscopy (PALS) and ultrasonic velocity obtained by Mathotra and Pethrick [24]. Following these results, it is reasonable to assume that inside the matrix of amorphous polymers, free volume with a more generalized notion, constituted from holes of varying sizes, is randomly distributed around polymer molecules. It will be shown that the way free volume is distributed inside the bulk matrix plays a decisive role to the material's macroscopic response. Following the experimental evidence provided by PALS [25] the radius distribution $f(R)$ is expressed as:

$$f(R) = 2\delta R\left[\cos\frac{2\pi R}{R+\delta R} - 1\right]\frac{\xi(1/\tau_3)}{(R+\delta R)^2} \tag{1}$$

where $\xi(1/\tau_3)$ is the inverse of the longest lifetime, δR expressing the thickness of an electron layer on the wall of a hole, estimated to be equal to 0.166 nm, and R is the radius of a spherical PALS free volume.

Then it is possible to obtain the free volume distribution as:

$$g(V) = \frac{f(R)}{4\pi R^2} \tag{2}$$

For a variety of glassy polymers Eq. (2) is represented with one characteristic peak, and is correlated with some materials characteristics, such as synthesis, curing schedule, thermal treatment, etc. [25].

In what follows, a free volume distribution function will be extracted, in the frame of statistical ensemble in thermodynamic equilibrium. The main assumption here is that in equilibrium state, above T_g, the macromolecules of a polymeric glass are in a state of random thermal motion. Some of these molecules may pull apart in such a way, as to open a void or a hole in the liquid.

In a rather simplified manner [26], it is assumed that each region of free volume comes in a spherical shape of radius R and that the energy of the free volume is equal to $E_R = 4\pi\gamma R^2$, where γ is the surface energy per unit area, almost equal to the surface energy of the liquid. According to the Boltzmann distribution, the possibility P for a macromolecule to neighbor with a hole of radius R at a certain position r is given by the expression:

$$P = c\exp\left[-\frac{E_R}{kT}\right] \quad \text{where} \quad E_R = 4\pi\gamma R^2 \tag{3}$$

where c is a constant, k is the Boltzmann constant and T is the temperature.

In analogy with statistical physics, where the Maxwell distribution of molecular speeds in an ideal gas [27], it can be extracted that the mean number of states (molecules) neighboring with holes with radius R between R and $R + \mathrm{d}R$ is given by:

$$F(R) = Nc4\pi R^2\exp\left(-\frac{4\pi\gamma R^2}{kT}\right) \tag{4}$$

where N is the number of states at positions with hole radius between R and $R + \mathrm{d}R$. The mean value of radius R can be easily extracted from Eq. (4) at the position where the first derivative of function $F(R)$ becomes zero:

$$\left.\frac{\mathrm{d}F(R)}{\mathrm{d}R}\right|_{R=\overline{R}} = 0 \Rightarrow \overline{R} = \frac{1}{2\sqrt{\pi\gamma/kT}} \tag{5}$$

Following Eq. (4), we can write in analogy, the free volume distribution function $g(V_\mathrm{f}) = F(R)/(4\pi R^2)$:

$$g\left(V_\mathrm{f}\right) = Nc\exp\left(-\frac{4\pi\gamma R^2}{kT}\right) \tag{6}$$

By setting $N = V_\mathrm{f}/\overline{V}_\mathrm{f}$ where $\overline{V}_\mathrm{f}$ is the mean value of the total free volume V_f, and considering that constant c of Eq. (6) can be calculated taking into account that the integration of the density probability function will be equal to unity, we have:

$$\int_0^\infty g\left(V_f\right)\mathrm{d}V_f = 1 \Rightarrow c\int_0^\infty \frac{V_\mathrm{f}}{\overline{V}_\mathrm{f}}\exp\left(-\left[\frac{V_\mathrm{f}}{\overline{V}_\mathrm{f}}\right]^{2/3}\right)\mathrm{d}V_\mathrm{f} = 1 \qquad (7)$$

Eq. (7) gives $c = 1/3\overline{V}_\mathrm{f}$, therefore the probability density function is given by:

$$g\left(V_\mathrm{f}\right) = \frac{1}{3}\frac{V_\mathrm{f}}{\left(\overline{V}_\mathrm{f}\right)^2}\exp\left(-\left[\frac{V_\mathrm{f}}{\overline{V}_\mathrm{f}}\right]^{2/3}\right) \qquad (8)$$

Eq. (8) is the probability density distribution function for the free volume of the liquid state. It is also assumed that this equation is valid in the glassy state as well, considering that this free volume distribution is established during the solidification process. The above procedure is presented in detail in Ref. [26].

We are referring now to a state of the representative volume V, where a strain field ε has been applied, high enough for plastic deformation to occur. The regions which are characterized with the largest amount of free volume, will be the most probable candidates for yield transition, that takes place at a critical strain $\overline{\varepsilon}$. The corresponding probability for this event to take place inside the material will be given by the following equation,

$$g(\varepsilon) = \frac{1}{3}\frac{\varepsilon}{(\overline{\varepsilon})^2}\exp\left(-\left[\frac{\varepsilon}{\overline{\varepsilon}}\right]^{2/3}\right) \qquad (9)$$

where $\overline{\varepsilon}$ expresses now the mean value of the distributed strain into the material. Applying this equation, the calculation of the number of sites which have been subjected to plastic transition, after strain ε has been imposed, is given by the following integral,

$$N(\varepsilon) = \int_0^\varepsilon \mathrm{d}\varepsilon\, g(\varepsilon) = \int_0^\varepsilon \frac{1}{3}\frac{\varepsilon}{(\overline{\varepsilon})^2}\exp\left(-\left[\frac{\varepsilon}{\overline{\varepsilon}}\right]^{2/3}\right)\mathrm{d}\varepsilon \qquad (10)$$

The above obtained integral can be further applied for the calculation of the rate of plastic strain deformation $\dot{\varepsilon}_y$ if we assume that each site is transformed to yield state by a constant rate $\dot{\kappa}$, which is calculated from the limited case of plastic saturation as $\dot{\kappa} = \dot{\alpha}/\alpha(\alpha_\mathrm{s}^\mathrm{m} - 1)$ [18]. The quantity $\alpha_\mathrm{s}^\mathrm{m}$ is the saturated stretch ratio and the corresponding saturated strain is obtained by dividing the stress with corresponding modulus in the post yield region, before strain hardening occurs.

The corresponding plastic strain rate equation will be given by the following formula,

$$\dot{\varepsilon}_y = \dot{\kappa}N(\varepsilon) = \frac{\dot{\alpha}}{\alpha\left(\alpha_\mathrm{s}^\mathrm{m} - 1\right)}\frac{1}{3}\int_0^\varepsilon \frac{\varepsilon}{(\overline{\varepsilon})^2}\exp\left(-\left[\frac{\varepsilon}{\overline{\varepsilon}}\right]^{2/3}\right)\mathrm{d}\varepsilon \qquad (11)$$

The value of the characteristic strain $\overline{\varepsilon}$, around which the above introduced distribution function works, is related with a specific microstructural parameter, expressing the strain above which no more elastic strain is developed.

3. Constitutive equations

As already mentioned, a number of factors strongly affect the yield behaviour of glassy state, namely strain rate, pressure, temperature as well as the thermal prehistory. Apart from this, when a constant strain below yield point is applied on amorphous polymers, the material undergoes a nonlinear viscoelastic behavior with a terminal stress below yield stress as well. These observations can give the impression that yield phenomenon in polymers is fundamentally different from that in metals that follow the yield criteria, and that it might be a special and unique nonlinear viscoelastic effect. Regarding the length scale of these viscoelastic and viscoplastic phenomena, some differences also are recorded, given that the characteristic size of shear bands associated with plastic phenomena is of the order of some micrometers [28,29] that exceeds three orders of magnitude the characteristic length of pure viscoelastic effect. What is true, however, is that these two phenomena coexist in the mechanical behavior of polymers [5], and is a matter of total strain and strain rate applied on the material which decides which of these two effects will be prevailed in respect to the other one. Matsuoka [30], who describes this behavior systematically in a relevant book, comes to the result that there is a critical strain ε^* which controls the viscoplastic response of glassy polymers. When the strain rate $\dot{\varepsilon}$ is slow $(\dot{\varepsilon}\tau_i < \varepsilon^*)$ where τ_i are a set of relaxation modes describing the viscoelastic behavior of polymers the yield stress σ_y is never reached and the final steady state stress is that of linear viscoelasticity equal to $E_i\tau_i\dot{\varepsilon}$, with E_i, the moduli of the corresponding modes. If the material exhibits no stress overshoot in the yield stress, then $\varepsilon^* = \dot{\varepsilon}\tau_i$, and the steady state stress is equal to the yield stress σ_y. When stress overshoot is observed, which is common in most glassy polymers, $\varepsilon^* < \dot{\varepsilon}\tau_i$, and beyond yielding, a transition takes place with a new structure in the material state, resulting to new smaller value of τ_i, which is equal to $\varepsilon^*/\dot{\varepsilon}$.

After a more detailed analysis, Matsuoka concluded that strain magnitude is a crucial factor in determining whether the viscoelastic or plastic path is followed. Regardless of transient or steady state conditions, it depends on whether $\varepsilon < \varepsilon^*$ or $\varepsilon > \varepsilon^*$.

This behavior according to Matsuoka can be approximated by a single Maxwell equation:

$$\sigma = E\varepsilon^*\left[1 - \exp\left(-\frac{\varepsilon}{\varepsilon^*}\right)\right] \qquad (12)$$

where E is the apparent modulus and ε is the viscoelastic strain. The estimation of critical strain ε^* can be made as follows: Most glassy polymers dilate under tensile stress by the amount $\Delta V/V \cong \varepsilon(1 - 2\nu)$, where ν is the Poisson ratio [30]. Making further the plausible assumption that at yielding the total volume change is related with the fractional free volume, and the corresponding strain is the critical strain ε^* of our analysis, it can be written that:

$$\varepsilon^* = \frac{\widehat{v}_\mathrm{f}}{1 - 2\nu} \qquad (13)$$

where $\widehat{v}_\mathrm{f}$ is the average value of fractional free volume.

Eq. (12) in combination with a kinematic formulation that separates the total deformation into plastic and elastic parts, proposed by Rubin [16,17] is used to describe the yield behaviour of the materials. This kinematic formulation is presented in detail elsewhere [18] for three dimensional problems. In the case of uniaxial deformation the time evolution of the elastic (viscoelastic) stretch ratio α_m is given by the expression:

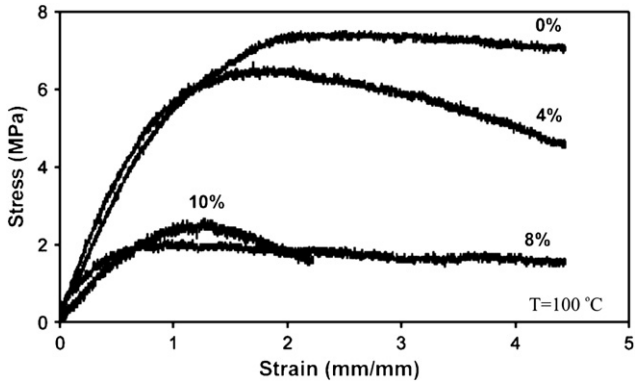

Fig. 1. Tensile stress–strain curves with a strain rate of 2.77×10^{-4} s^{-1}, at 100 °C, for all materials tested.

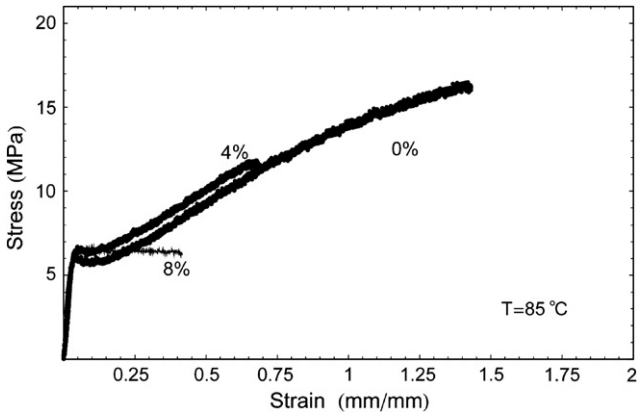

Fig. 2. Tensile stress–strain curves with a strain rate of $2.77 \times 10^{-4}\ s^{-1}$, at 85 °C, for all materials tested.

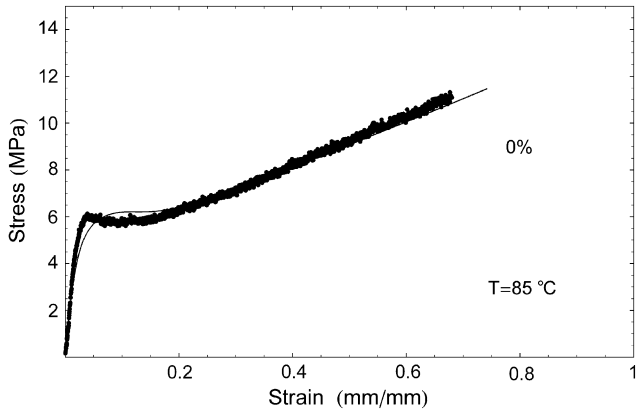

Fig. 4. Tensile stress–strain curves with a strain rate of $2.77 \times 10^{-4}\ s^{-1}$, at 85 °C, for pure PS. Thick lines: experimental data, thin lines: simulated results.

$$\frac{\dot{\alpha}_m}{\alpha_m} = \left[\frac{1+\frac{1-2\nu}{2(1+\nu)}\left(\frac{\alpha_m^3-1}{\alpha_m}\right)}{1+\frac{1-2\nu}{6(1+\nu)}\left(\frac{5\alpha_m^3-2}{\alpha_m}\right)}\right] \times \left[\frac{\dot{\alpha}}{\alpha} - \frac{\dot{\varepsilon}_y}{18}\left(\frac{\alpha_m^3-1}{\alpha_m^3}\right)\left(4\alpha_m^3+2\right)\right] \tag{14}$$

with the initial condition $\alpha_m(0)=1$, ν is the Poisson ratio and $\dot{\alpha}$ is the imposed strain rate. It must be mentioned that the stretch ratio α is equal $(1-\varepsilon)$ in compression deformation tests and $\dot{\varepsilon}_y$ is the rate of plastic deformation as it was specified earlier and expressed by Eq. (11).

4. Application on the viscoplastic response of a polymer nanocomposite

4.1. Experimental

The tensile and compressive behaviour of polymer nanocomposites, based on Polystyrene (PS) and silica nanoparticles (type Silica Aerosil R972), at 4, 8 and 10% per weight, will be simulated through the proposed analysis. Given that these materials exhibit a brittle behaviour at room temperature, the experimental results at higher temperatures namely 85 and 100 °C will be examined. Tensile tests were carried out with an Instron 1121 type tester, with dumbbell type specimens, according to ASTM D 638, and at an effective strain rate of $2.77 \times 10^{-4}\ s^{-1}$. The tests were performed with a high temperature chamber series 3119-406 of Instron Ltd. The corresponding results are presented in detail in Ref. [31]. Moreover, in the present work, compressive experiments were performed at 85 °C for a more systematic analysis of the materials under investigation. Cylindrical specimens with a mean diameter of 10 mm and a height/diameter ratio equal to 1 were used. The effective strain rate was $2.5 \times 10^{-3}\ s^{-1}$. Nominal strain measurements in all cases were obtained, as no extensometer could be applied due to the presence of chamber. The experimental results for tension at 100 °C, and tension and compression at 85 °C are presented in Figs. 1–3 correspondingly.

4.2. Results and discussion

At 100 °C, which is a temperature above T_g, the nanoparticles do not have any contribution to the mechanical response of the material. This fact is reflected from Fig. 1 where the initial slope of the stress–strain curves is almost the same for pure PS and PS-4%. Also the observed behaviour is a pure viscoelastic one, exhibiting a steady state stress σ_{ss} equal to $E\tau\dot{\varepsilon}$, where E is the apparent modulus, $\dot{\varepsilon}$ the imposed strain rate and τ is a mean relaxation time [30].

The higher nanosilica content, however (PS-8%, PS-10%), seems to have a deterioration effect on the mechanical response at this temperature. This fact means that particles and mainly particle-agglomerates act as holes, leading to a small reduction in the load bearing cross-section of the sample. For the sample PS-4% it may be concluded that a better dispersion quality has been created.

Figs. 2 and 3 demonstrate the tensile and compressive stress–strain curves at 85 °C correspondingly. It is observed from Fig. 2 that at 85 °C which is a temperature close but below T_g, the materials exhibit a viscoplastic behaviour, with a stress peak at

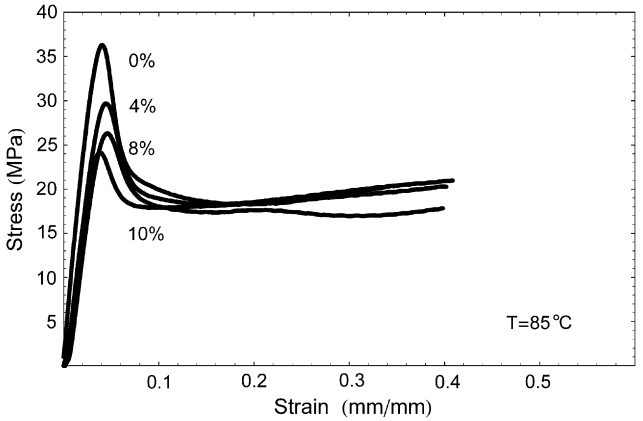

Fig. 3. Compressive stress–strain curves with a strain rate of $2.5 \times 10^{-3}\ s^{-1}$ at 85 °C, for all materials tested.

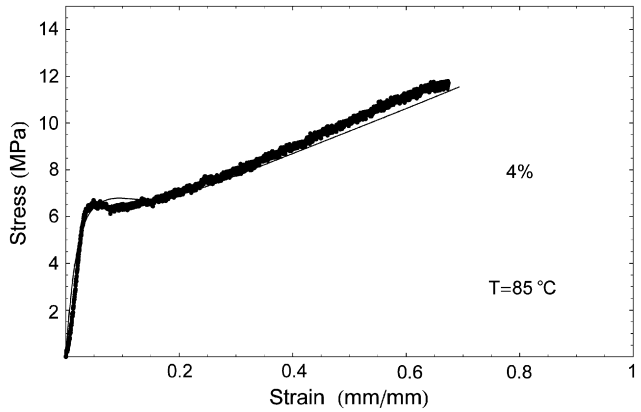

Fig. 5. Tensile stress–strain curves with a strain rate of $2.77 \times 10^{-4}\ s^{-1}$, at 85 °C, for PS–4%$SiO_2$. Thick lines: experimental data, thin lines: simulated results.

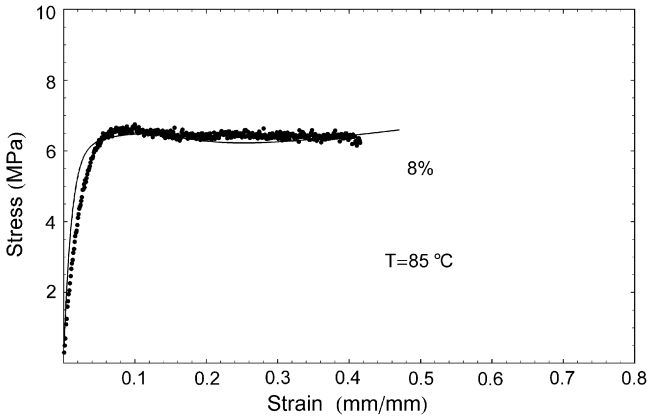

Fig. 6. Tensile stress–strain curves with a strain rate of 2.77×10^{-4} s^{-1}, at 85 °C, for PS–8%SiO_2. Thick lines: experimental data, thin lines: simulated results.

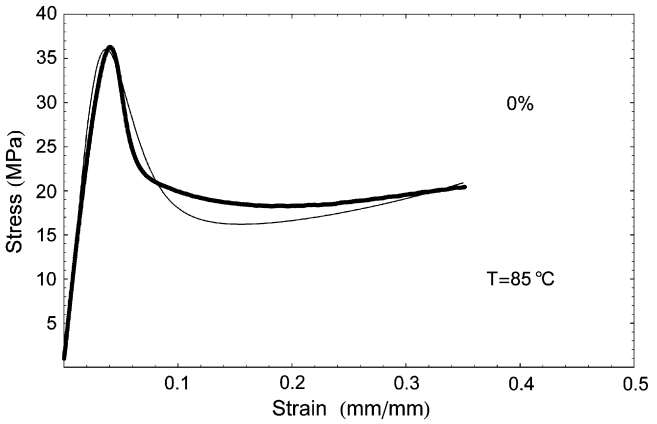

Fig. 8. Compressive stress–strain curves with a strain rate of 2.5×10^{-3} s^{-1}, at 85 °C, for pure PS. Thick lines: experimental data, thin lines: simulated results.

yielding, followed by a strain softening and hereafter a strain hardening. The initial slope of stress–strain curves is slightly increased as filler weight fraction is increased, while this trend is reversed at 10%. Similar trend is also observed in yield stress, showing a relatively higher value at 4% and lower values for the other two filler contents.

In Fig. 3 the corresponding compressive stress–strain curves are shown, exhibiting a sharp stress overshoot at yielding, followed by an intense strain softening and slight strain hardening at higher strains. The initial slope seems not to be greatly affected as filler content increases, while yield stress is monotonically decreased [32]. This behaviour is not typical in conventional particulate composites, where yield stress is enhanced due to filler's presence. Also, concerning compressive behaviour, there are no experimental data available for polymeric nanocomposites.

The experimental data as presented above will be analyzed and simulated by implementation of the proposed model. As it has been discussed, two main factors affect the yield behaviour of polymeric structure, namely the accumulated strain (in respect to the imposed strain rate) and the distributed nature in terms of various types of defects into the polymeric bulk. Considering that a number of free volume holes and/or other type defects are distributed into the material, the imposed strain will be installed preferably in those regions. Therefore, the onset of yielding will be facilitated in the localized regions with extra free volume or higher density fluctuations. Consequently, it is an interesting task to study further how the presence of nanoparticles affects the yield behaviour of polymers.

It is generally accepted that a nanoparticle will perturb the conformation of the polymeric matrix around it, and it is a matter of interest, whether such conformational changes are directly responsible for the mechanical behaviour of the polymer [33]. The presence of silica nanoparticles leads to the development of additional localized regions with different size and extent. When the dispersed particles preserve the nanoscale size, which is of the same order of radius of gyration of the macromolecules and the interface width, some kind of better homogeneity might occur. Therefore, one of the mechanisms through which nanoparticles reinforce glassy polymers, is by reducing the degree of mechanical inhomogeneity, that arises at nanometer length scales. Less inhomogeneity would render the composite material not only stronger but also more resistant to failure.

Due to these postulations, the values of the model parameters, namely the mean value $\bar{\varepsilon}$ of the distribution density function for strain inhomogeneity Eq. (11) and the characteristic strain ε^*, may support enough evidence to extract some interesting conclusions about the micromorphology of the materials tested.

More specifically, ε^* is directly related with the mean size of various types of defects; so it is expected to increase with increasing filler weight fraction. On the other hand, mean value $\bar{\varepsilon}$ is connected with the average amount of elastic strain that is imposed into the material at the onset of yielding, or equivalently, expresses the strain above which no more elastic strain is developed. As discussed earlier, this parameter value is similar with the saturated elastic strain $1 - \alpha_s^m$. Therefore, its value can be estimated by

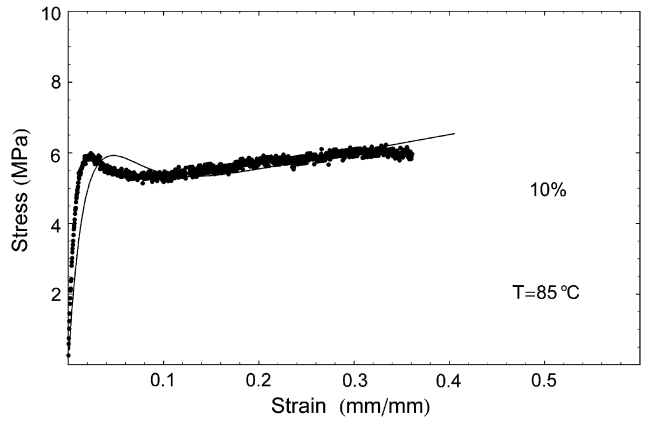

Fig. 7. Tensile stress–strain curves with a strain rate of 2.77×10^{-4} s^{-1}, at 85 °C, for PS–10%SiO_2. Thick lines: experimental data, thin lines: simulated results.

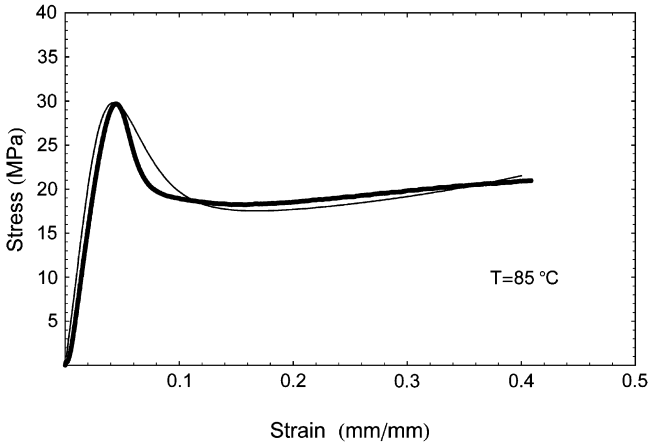

Fig. 9. Compressive stress–strain curves with a strain rate of 2.5×10^{-3} s^{-1}, at 85 °C, for PS–4%SiO_2. Thick lines: experimental data, thin lines: simulated results.

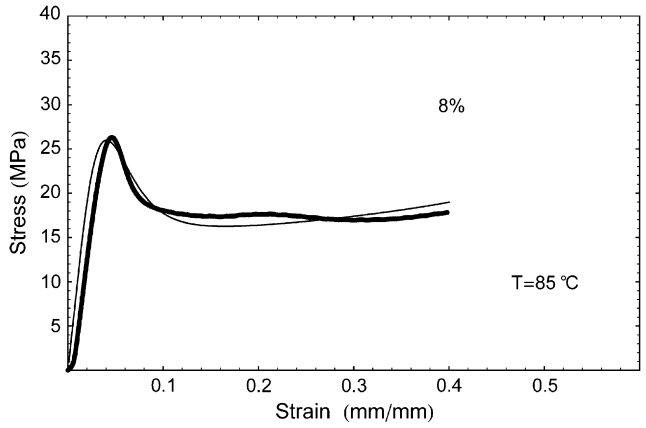

Fig. 10. Compressive stress–strain curves with a strain rate of $2.5 \times 10^{-3}\ s^{-1}$, at 85 °C, for PS–8%$SiO_2$. Thick lines: experimental data, thin lines: simulated results.

dividing the almost stable value of stress, establishing after strain softening, by the apparent modulus.

To further model the strain hardening, the concept of back stress will be used, which expresses the resistance the material overcomes, due to the molecular alignment after yielding. This alignment is related with changes in the configurational entropy of the system. Back stress tensor introduced in Ref. [5] is expressed here by a neohookean equation in simple extension:

$$\sigma_h = C_r\left(\lambda - \frac{1}{\lambda^2}\right) \tag{15}$$

Where λ is the plastic stretch ratio in the loading direction, with $\lambda = 1 + \alpha - \alpha_m$ and C_r is the rubbery modulus. The simulation of the experimental data has been performed as follows: Combining Eqs. (11) and (14), and making the integration in Eq. (14), the elastic strain equal to $\alpha_m - 1$ is obtained. Hereafter, it is combined with the constitutive Eq. (12) for the stress calculation. To formulate the strain hardening, the total stress is extracted by the further addition of σ_h of Eq. (15). Due to the complexity of equations, numerical integration of Eq. (14) using small time steps in the frame of the software Mathematica [34] were made and finally the stress–strain curves of Figs. 2 and 3 were simulated, and are presented as solid lines in Figs. 4–7 for tension and Figs. 8–11 for compression. From these plots, a satisfactory agreement between theory and experiments in all cases is testified. The model parameter values are summarized in Table 1. Modulus E of Eq. (12) was equal to 1079 MPa, and the Poisson ratio was considered as $\nu = 0.3$, assuming that the filler's presence does not strongly affect it. For

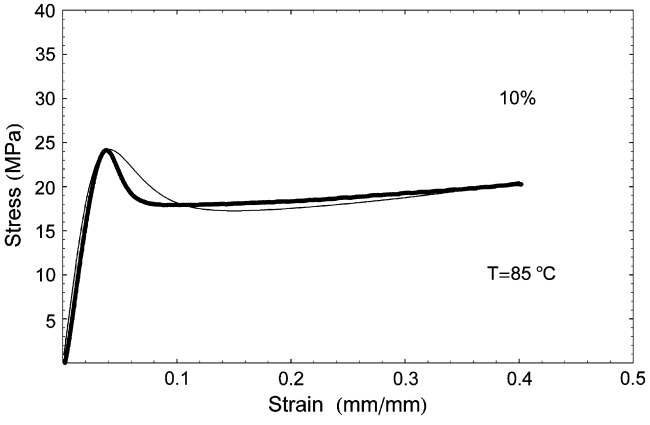

Fig. 11. Compressive stress–strain curves with a strain rate of $2.5 \times 10^{-3}\ s^{-1}$, at 85 °C, for PS–10%$SiO_2$. Thick lines: experimental data, thin lines: simulated results.

Table 1
Model parameter values

Sample	ε^*	$\bar{\varepsilon}$	α_m^s	C_r (MPa)
PS	0.035	0.008	1.008	3
PS–4%SiO_2	0.043	0.008	1.008	3
PS–8%SiO_2	0.055	0.007	1.007	2
PS–10%SiO_2	0.07	0.006	1.006	2.3

both types of deformation, tension and compression, analogous parameter values with the same trend, in respect to filler weight fraction, were found to simulate all the specific features of the experimental data. We only need to change the average initial slope of the stress–strain curves, applying a higher value for compression, due to pressure effect.

The critical strain ε^* was increased for increasing filler content, expressing this way, the increased average size of defects, developed as a consequence of the nanoparticle's dispersion. On the other hand, mean value $\bar{\varepsilon}$ exhibits a slight decrement in respect to filler content. The relative variation of model parameters $\varepsilon^*, \bar{\varepsilon}$ with filler content is reasonable and compatible with the basic model assumptions. Therefore, as filler weight fraction increases, the greater defect's size (higher ε^*) facilitates the onset of yielding, and a lower distributed mean strain $\bar{\varepsilon}$ is required for the plastic transition of the localized regions.

5. Conclusions

In the present work, the yield effect of glassy state and the complementary effect of strain softening are discussed with a unified approach. A free volume distribution function is introduced, based on equilibrium thermodynamics, which is further treated as a strain distribution density function, due to the strain localization and strain non-uniformity under loading conditions. This function is combined with a proper kinematic formulation for the separation of strain into plastic and viscoelastic part. Tensile and compressive experimental data for PS and PS/SiO_2 nanocomposites were used to test the model validity. Model parameters, the same for both types of deformation, were reasonably varied for various material types, expressing the existence of higher average size defects due to the presence of nanofillers.

References

[1] Bowden PB, Raha S. Phil Mag 1974;29:149–66.
[2] Robertson RE. J Chem Phys 1966;44:3950–6.
[3] Argon AS. Phil Mag 1973;28:839–65.
[4] G'Sell C, Jonas JJ. J Mater Sci 1982;14:583.
[5] Boyce MC, Parks DM, Argon AS. Mech Mater 1988;7:15.
[6] Hasan OA, Boyce MC. Polymer 1993;34:5085–92.
[7] Hasan OA, Boyce MC. Polym Eng Sci 1995;35:331–44.
[8] Hasan OA, Boyce MC, Li XS, Berko S. J Polym Sci Part B Polym Phys 1993;31:185–97.
[9] Haward RN, Young RJ. The physics of glassy polymers. New York: Chapman and Hall; 1997.
[10] Eyring HJ. J Chem Phys 1936;4:283.
[11] Dlubek G, Bondarenko V, Pionteck J, Supej M, Wutzler A, Krause-Rehberg R. Polymer 2003;44:1921.
[12] Schmidt M, Maurer FHJ. Polymer 2000;41:8419.
[13] Kanaya T, Tsukushi T, Kaji K, Bartos R, Kristiak J. Phys Rev E 1999;60(2):1906–12.
[14] Higuchi H, Yu Z, Jamieson AM, R.Simha R, McGervey JD. J Polym Sci Part B Polym Phys 1995;33:2295.
[15] Wang XY, Lee KM, Lu Y, Stone MT, Sanchez IC, Freeman BD. Polymer 2004;45:3907.
[16] Rubin MB. Int J Solids Struct 1994;31(19):2615.
[17] Rubin MB. Int J Solids Struct 1994;31(19):2635–52.
[18] Spathis G, Kontou E. Polymer 1998;39:135–42.
[19] Spathis G, Kontou E. J Appl Polym Sci 1999;71:2007.
[20] Wendorff JH, Fisher EW, Kolloid ZZ. Polymer 1973;251:876.
[21] Curro JJ, Roe RJ. Polymer 1984;25:1424–30.
[22] Roe RJ, Curro JJ. Macromolecules 1983;16:428–34.
[23] Williams ML, Landel RF, Ferry JD. J Am Chem Soc 1955;77:3701–7.

[24] Malhotra BD, Pethrick RA. Polymer 1983;24:165.
[25] Goyanes S, Rubiolo G, Salgueiro W, Somoza A. Polymer 2005;46:9081.
[26] Spathis G. J Mater Sci, in press.
[27] Reif F. Statistical physics, vol. 5. New York: Mc Graw Hill; 1965.
[28] Eckard C. Phys Rev 1984;73:373.
[29] Besseling JF. Proceedings of IUTAM symposium on irreversible aspects of continuum mechanics. Vienna: Springer; 1968. p. 16-53.
[30] Matsuoka S. Relaxation phenomena in polymers. 2nd ed. Hanser; 1992.
[31] Kontou E, Anthoulis G. J Appl Polym Sci 2007;105:1723–31.
[32] Truss RW, Lee AC. Soc Chem Industry Polymer Int 2003;52:1790–4.
[33] Papakonstantopoulos G, Yoshimoto K, Doxastakis M, Nealy PF, de Pablo J. Phys Rev E 2005;72:031801.
[34] Wolfram S. Mathematica, a system for doing mathematics by computer. 4th ed. New York: Wolfram Research; 1999.